0888-8809/05/$15.00/0
Printed in U.S.A.

Molecular Endocrinology 19(1):90–101

doi: 10.1210/me.2004-0153

The Orphan Receptor Tyrosine Kinase Ror2 Modulates Canonical Wnt Signaling in Osteoblastic Cells

Julia Billiard, Deana S. Way, Laura M. Seestaller-Wehr, Robert A. Moran, Annamarie Mangine, and Peter V. N. Bodine

Women's Health Research Institute, Wyeth Research, Collegeville, Pennsylvania 19426

Ror2 is an orphan receptor tyrosine kinase that plays crucial roles in developmental morphogenesis, particularly of the skeleton. We have identified human Ror2 as a novel regulator of canonical Wnt signaling in osteoblastic (bone-forming) cells with selective activities, enhancing Wnt1 but antagonizing Wnt3. Immunoprecipitation studies demonstrated physical interactions between human Ror2 and mammalian Wnt1 and Wnt3. Functionally, Ror2 antagonized Wnt1- and Wnt3-mediated stabilization of cytosolic β-catenin in osteoblastic cells. However, Ror2 had opposing effects on a more distal step of canonical Wnt signaling: it potentiated Wnt1 activity but inhibited Wnt3 function as assessed by changes in Wnt-responsive reporter gene activity. Despite binding to Ror2, neither Wnt1 nor Wnt3 altered receptor activity as assessed by levels of Ror2 autophosphorylation. The ability of Ror2 to regulate canonical Wnt signaling in osteoblastic cells should have physiological consequences in bone, because Wnt signaling is known to modulate osteoblast survival and differentiation. Expression of *Ror2* mRNA was highly regulated in a biphasic manner during human osteoblast differentiation, being virtually undetectable in pluripotent stem cells, increasing 300-fold in committed preosteoblasts, and disappearing again in osteocytes. Furthermore, Ror2 expression in osteoblasts was suppressed by the Wnt antagonist, secreted frizzled-related protein 1. The regulated expression of Ror2 during osteoblast differentiation, its inverse expression pattern with secreted frizzled-related protein 1, and its ability to modulate Wnt signaling in osteoblastic cells suggest that Ror2 may regulate bone formation. (*Molecular Endocrinology* 19: 90–101, 2005)

ROR2 BELONGS TO a family of orphan receptor tyrosine kinases that in mammals consists of two members, Ror1 and Ror2. Ror receptors are most closely related to Trk neurotropin receptors and muscle-specific kinase (1). During mouse development, Rors are expressed in many tissue types including face, limbs, heart, brain, and lungs (2–4).

Mice lacking Ror2 exhibit dwarfism, short limbs and tails, facial abnormalities, ventricular septal defects, and respiratory dysfunction resulting in neonatal lethality (5–7). In humans, mutations within the *Ror2* gene are responsible for brachydactyly type B, characterized by hypoplasia/aplasia of distant phalanges, and for Robinow syndrome characterized by short stature, limb bone shortening, segmental defects of the spine, and a dysmorphic facial appearance (8–12). Thus, Ror2 plays important roles in developmental morphogenesis, in particular in skeletal development.

Wnts are secreted glycoproteins that mediate fundamental biological processes such as embryogenesis, morphogenesis, and tumorigenesis (13, 14). They bind to a membrane receptor Frizzled (FZ) and a coreceptor, the low-density lipoprotein receptor-related protein (LRP) and activate either the canonical β-catenin pathway or one of at least two noncanonical pathways (15, 16). Which of the pathways gets activated depends on the Wnt, FZ receptor, and the cell type involved, with Wnt1 subfamily (*e.g.* Wnt1, Wnt3, Wnt3a, Wnt8) activating the canonical pathway, and Wnt5a subfamily (*e.g.* Wnt5a, Wnt11) activating the noncanonical pathways. Signaling through the canonical pathway depends on the levels of β-catenin in the cell (reviewed in Ref. 15). Wnt binding to its membrane receptor complex leads to inhibition of glycogen synthase kinase-3β and subsequent stabilization of β-catenin that translocates to the nucleus, where it binds to and activates lymphoid-enhancer binding factor/T cell transcription factors (TCF).

In osteoblasts, Wnt signaling mediates cell survival and differentiation (17). Loss-of-function mutations in the coreceptor of the canonical Wnt signaling, low-density lipoprotein receptor related protein (LRP5), cause a defect in bone accrual in humans that leads to a low peak bone mass and premature fractures [os-

First Published Online September 23, 2004

Abbreviations: AP, Alkaline phosphatase; CMV, cytomegalovirus; CRD, cysteine-rich domain; FZ, frizzled; β-gal, β-galactosidase; HA, hemagglutinin; HI FBS, heat-inactivated fetal bovine serum; hMSC, human mesenchymal stem cell; HOB, human osteoblastic cell line; LRP, lipoprotein receptor-related protein; PS, penicillin-streptomycin; Ror2KD, Ror2 kinase domain; sFRP1, secreted frizzled-related protein 1; TCF, T cell transcription factor.

***Molecular Endocrinology* is published monthly by The Endocrine Society (http://www.endo-society.org), the foremost professional society serving the endocrine community.**

teoporosis pseudoglioma syndrome (18)]. Disruption of *LRP5* gene in mice results in suppressed osteoblast proliferation and activity that leads to diminished bone formation and trabecular bone volume (19). In addition, mice lacking a Wnt antagonist secreted frizzled-related protein 1 (sFRP1) exhibit diminished osteoblast and osteocyte apoptosis, increased osteoblast activity, proliferation and differentiation, and increased trabecular bone mineral density and volume (20).

The Ror receptors contain an intracellular tyrosine kinase domain and an extracellular cysteine-rich domain (CRD) that resembles the Wnt binding sites of FZ proteins (21, 22). Recently, the ectodomain of *Xenopus* Ror2 has been shown to bind *Xenopus* Wnt7, Wnt8, and Wnt11 (23) and to inhibit convergent extension in *Xenopus* embryos, at least in part, through stimulation of the noncanonical Wnt signaling (23). In mammals, the extracellular domain of the mouse Ror2 has been demonstrated to bind mouse noncanonical Wnt5a (24). In addition, the phenotypes of Ror2$-/-$ and Wnt5a$-/-$ mice are strikingly similar, and Ror2 potentiates Wnt5a-induced activation of c-Jun N-terminal kinase in cultured cells, suggesting that it may be involved in noncanonical Wnt signaling in mammals (24).

Here we identify Ror2 in a gene chip array analysis of the late stages of human osteoblast differentiation as a gene whose expression is significantly downregulated between preosteoblasts and osteocytes. We then show that Ror2 expression is virtually undetectable in pluripotent stem cells but increases 300-fold in preosteoblasts before declining in osteocytes. Furthermore, we find that Ror2 expression is downregulated by a Wnt antagonist sFRP1. We show that Ror2 physically interacts with canonical Wnts, Wnt1 and 3, and inhibits Wnt-mediated stabilization of cytosolic β-catenin. However, Ror2 has opposing effects on a more distant step of Wnt signaling in osteoblastic cells: Wnt-induced promoter activation, where it potentiates Wnt1, but inhibits Wnt3-mediated activation of TCF DNA-binding elements. Wnt1 potentiation and the majority of Wnt3 inhibition require the tyrosine kinase activity of the Ror2 receptor. Because Wnt is a key mediator of osteoblast survival, the ability of Ror2 to differentially regulate Wnt activity may have complex effects on bone formation.

RESULTS

We have previously developed a collection of conditionally immortalized adult human osteoblastic cell lines (HOB cells) representing different stages of differentiation, including preosteoblasts, early and late osteoblasts, and preosteocytes (25). We subsequently performed gene chip analysis of polyA$^{(+)}$ RNA from these cell lines on the Affymetrix Hu6800 chip and the custom-made GIHuman1a chip enriched in bone and cartilage cDNAs (26). Forty-seven genes were identified, the expression of which changed 3-fold or more on both chips between preosteoblastic and preosteocytic stages (26); but this analysis excluded the transcripts for which probes were present on only one chip, but not the other. We have now analyzed these transcripts and found several mRNAs the expression of which changed 3-fold or more between preosteoblasts and preosteocytes on the chip that reported their expression. One of these transcripts encoded the Ror2 kinase that attracted our attention, because it contains a CRD domain that has been shown in other proteins to bind Wnt growth factors that are critically important for osteoblast proliferation, differentiation, and survival. The Ror2 probes were present on the GIHuman1a chip, and on this chip Ror2 expression decreased 5-fold between preosteoblasts and preosteocytes. We confirmed and extended this result by real-time RT-PCR using total cellular RNA from preosteoblasts (cell line HOB-03-C5), early and late osteoblasts (HOB-02-C2 and HOB-02-C1), preosteocytes (HOB-01-C1), and osteocytes (HOB-05-T1). Evidence demonstrating that these HOB cell lines indeed represent the corresponding stages of differentiation has been summarized previously (25). As shown in Fig. 1A, Ror2 expression was highest in preosteoblasts, decreased in early osteoblasts, increased in late osteoblasts, and then declined steadily as cells progressed to osteocytes. Real-time RT-PCR showed that expression of Ror2 gene in untransformed adult human osteoblasts was closest to the early osteoblast in our HOB model (Fig. 1A). Both gene chip analysis (data not shown) and real-time RT-PCR (Fig. 1A) revealed that expression of the other Ror family member, Ror1, decreased about 2-fold between preosteoblasts and osteoblasts and remained at this level for the remaining stages of differentiation.

We next looked at expression of the Ror kinases during early stages of differentiation from pluripotent stem cells to committed preosteoblasts. We treated human mesenchymal stem cells (hMSCs) with growth medium or osteogenic medium for up to 21 d as described in *Materials and Methods* and monitored their alkaline phosphatase (AP) activity and osteocalcin secretion. During this time, the AP activity and osteocalcin secretion in cells exposed to growth medium remained undetectably low (data not shown). In contrast, in cells treated with osteogenic cocktail, the AP activity rose gradually during the first 21 d, but the osteocalcin expression remained undetected (Fig. 1B, *inset*), confirming differentiation from stem cells to preosteoblasts. Ror2 expression was virtually undetectable before the onset of differentiation and remained unchanged when cells were incubated in growth medium (data not shown). However, as is shown in Fig. 1B, Ror2 expression increased more than 300-fold in cells exposed to osteogenic medium, whereas Ror1 expression remained unchanged. Thus, Ror2 expression increases during early stages of osteoblast differentiation, peaks in committed proliferat-

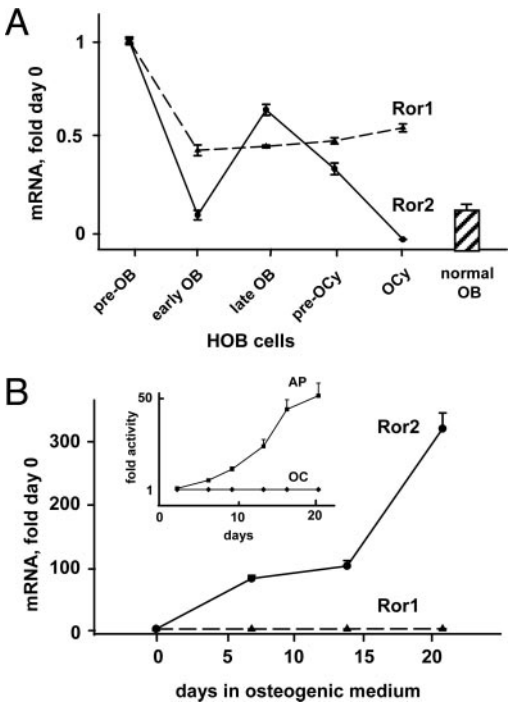

Fig. 1. Ror2 Expression Peaks in Committed Preosteoblastic Cells

A, Expression of Ror2 (*solid line, circles*) and Ror1 (*dashed line, triangles*) in human cell lines representing late stages of osteoblast differentiation. *Hatched bar* shows the level of Ror2 expression in primary human osteoblasts. OB, Osteoblasts; OCy, osteocytes. B, Expression of Ror2 (*solid line, circles*) and Ror1 (*dashed line, triangles*) in early differentiation of hMSC treated with osteogenic medium for the indicated time. *Inset*: Alkaline phosphatase (AP) activity and osteocalcin (OC) secretion in the same cells. Both were assessed as described in *Materials and Methods*, and values observed at d 0 were set at 1. In A and B the expression of Ror genes was assessed by real-time RT-PCR as described in *Materials and Methods* using probes and primers listed in Table 1, and the levels of mRNA were normalized to the expression of 18S rRNA in each sample. The relative mRNA expression in preosteoblastic cells (A) and before addition of osteogenic medium (B) was set at 1. The data are presented as means ± SE of at least three RT-PCRs per point; the figure shows representative traces of at least two independent experiments.

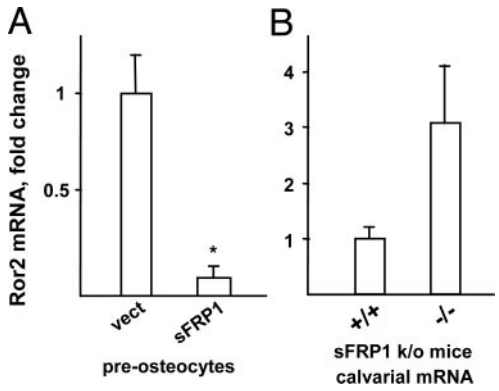

Fig. 2. sFRP1 Suppresses Ror2 Expression

Results of the real-time RT-PCR analysis of Ror2 expression in conditionally immortalized preosteocytes stably overexpressing empty vector or sFRP1 (A) and from calvarial bones of wild-type (+/+) or sFRP1 −/− mice (B). The relative mRNA expression in the vector-expressing cells and in wild-type mice was set at 1. In A, three empty vector clones and five independent sFRP1-overexpressing clones were analyzed, and the results are presented as means ± SE. The *asterisk* indicates significant changes from empty vector clones ($P < 0.001$). Panel B shows means ± SD of two mice per group. Real-time RT-PCR was performed as described in *Materials and Methods* using probes and primers listed in Table 1, and the levels of mRNA were normalized to the expression of glyceraldehyde-3-phosphate dehydrogenase mRNA in each sample.

ing preosteoblasts, and then declines during terminal osteocytic differentiation.

We have previously shown that an antagonist of Wnt signaling sFRP1 promotes osteoblast apoptosis (27) and that mice engineered to lack sFRP1 have increased bone formation (20). Here we used real-time RT-PCR to analyze Ror2 expression in HOB preosteocytic cells stably overexpressing sFRP1 or control vector. We examined three control clones and five sFRP1 clones ranging in overexpression from 7- to 1500-fold and found that Ror2 expression was strongly suppressed in all sFRP1 clones examined (Fig. 2A). Gene chip analysis (data not shown) and real-time RT-PCR (Fig. 2B) further demonstrated that calvariae of sFRP1 knockout mice expressed 3-fold more Ror2 message than did the wild-type controls, revealing a reciprocal relationship between expression of a Wnt antagonist sFRP1 and Ror2. In contrast, there was no difference in Ror1 expression between control and sFRP1-overexpressing clones or between wild-type and sFRP1-null mice (data not shown).

To begin to assess the role of Ror proteins in osteoblast physiology, we cloned human Ror1 and Ror2 in collaboration with Invitrogen Corporation. Our clones differed from sequences reported in GenBank by several substitutions. Substitutions in Ror1 sequence (accession no. NM_005012) were T1928C (M518T) and A3107G (K911R); substitutions in Ror2 sequence (accession no. NM_004560) were C2287T (silent) and G2654A (V819I). To date, most of the work in the field has been done with nonhuman Ror clones. However, when transfected into mammalian cells, our Ror2 clone produced a functional kinase of expected molecular weight as previously reported with the GenBank sequences of human Ror2 (28).

Next, we generated expression plasmids shown in Fig. 3A for full-length Ror1 and Ror2 and for several Ror2 mutants, each containing a COOH-terminal flag epitope tag for protein identification. In the Ror2 kinase domain (Ror2KD) mutant, three lysines at positions 504 (in the putative ATP binding domain), 507, and 509 were replaced with isoleucines (23). In the Ror2ΔCRD mutant, the entire CRD domain except for the last residue (C300) was deleted in frame. All ex-

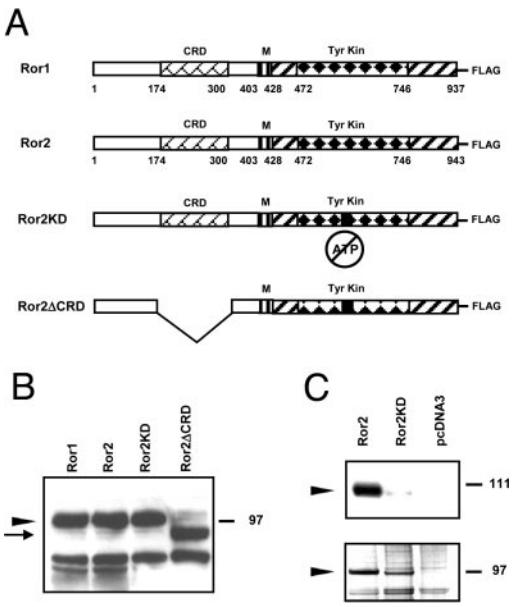

Fig. 3. Expression of Ror Proteins in U2OS Cells

A, Schematic representations of the full-length Ror1 and Ror2 kinases and the Ror2 mutants described in the text. FLAG, Flag epitope tag; CRD, cysteine-rich domain; M, transmembrane domain; Tyr Kin, tyrosine kinase domain. B, Western immunoblot for the flag epitope tag of the whole-cell protein extracts (30 μg/lane) from U2OS cells transfected with the indicated Ror constructs. Ror1, Ror2, and Ror2KD are marked by an *arrowhead*; Ror2ΔCRD is marked by an *arrow*. C, The *top panel* shows an autoradiograph of the results of *in vitro* autophosphorylation assay performed as described in *Materials and Methods* using Ror2 or Ror2KD immunoprecipitated on flag affinity agarose. In the *bottom panel*, 10% of the flag-immunoprecipitated proteins were separated by SDS-PAGE and analyzed by silver staining to assess kinase levels in the autophosphorylation reactions.

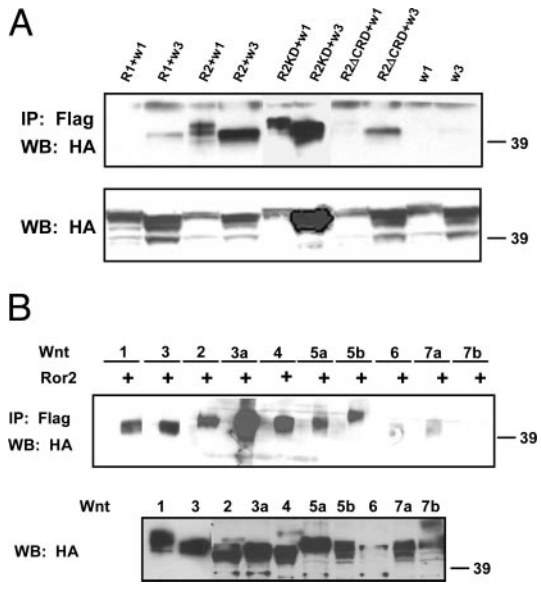

Fig. 4. Analysis of Ror-Wnt Binding

A, U2OS cells were transiently transfected with the indicated Ror (R) constructs tagged with flag epitope tag and HA-tagged Wnts (W). The total amount of DNA was kept constant by addition of pcDNA3.1(+) in place of Rors. At 24–48 h, lysates were analyzed by SDS-PAGE directly (*bottom*) or after immunoprecipitation with antiflag antibody (*top*). Immunoblotting was performed with anti-HA antibody. B, COS7 cells were transiently transfected with the indicated Wnts-HA and Ror2-Flag (+) or pcDNA3.1. At 24 h, lysates were immunoprecipitated with antiflag antibody and analyzed for the presence of Wnts by anti-HA antibody (*top*). The *bottom panel* shows Western blot analysis with anti-HA antibody of the COS7 extracts containing the indicated Wnts and the Ror2-flag (control for equal loading in the immunoprecipitation reactions).

pression plasmids were transiently transfected into U2OS osteosarcoma cells that do not have endogenous Ror expression as assessed by real-time RT-PCR (data not shown). Western immunoblotting with antiflag antibody showed that all Ror proteins express at similar levels in U2OS cells (Fig. 3B). Both Ror2 and Ror2KD could be precipitated out of U2OS extracts on flag affinity agarose (Fig. 3C, *bottom panel*). The immunoprecipitated Ror2, but not Ror2KD mutant, could phosphorylate itself *in vitro* in the presence of ^{32}P-ATP (Fig. 3C, *top panel*) confirming that Ror2KD has lost its kinase activity.

To assess whether human Rors bind canonical Wnts, we performed immunoprecipitation experiments with lysates of U2OS cells cotransfected with flag-tagged Rors and hemagglutinin (HA)-tagged Wnts. Antiflag affinity agarose was used for immunoprecipitation followed by immunoblotting with anti-HA antibody. Equal levels of precipitation of different Ror proteins were verified by immunoblotting with antiflag antibody (data not shown). As shown in Fig. 4A, under our experimental conditions, Ror1 did not precipitate Wnt1 and precipitated Wnt3 very weakly. However, both Wnt1 and Wnt3 were immunoprecipitated in complexes with Ror2. The specificity of interactions was demonstrated by the fact that antiflag antibody failed to immunoprecipitate Wnts in the absence of Ror2 coexpression. Loss of kinase activity did not affect the ability of Ror2 to bind Wnt1 or Wnt3 (Fig. 4A). As expected, deletion of the CRD domain that mediates Wnt binding of FZ receptors (29, 30) completely abolished Wnt1 binding to the Ror2 receptor (Fig. 4A). However, the Ror2ΔCRD mutant retained some of its Wnt3 binding capacity (Fig. 4A). On average, 30% of Wnt3 binding was retained by the Ror2ΔCRD mutant in three independent experiments (see *Discussion*).

To address the specificity of Ror2-Wnt interactions, we performed the immunoprecipitation experiment with a panel of different Wnt proteins (Fig. 4B). In this experiment, ten different HA-tagged Wnts were overexpressed in COS7 cells in the absence or presence of Ror2. As is shown in Fig. 4B, we observed the best binding of Ror2 to Wnt3a, followed by Wnt3, -4, -2, -1, -5b, and -5a. Ror2 bound Wnt6 and 7a only weakly, although Wnt6 expression in COS7 cells was not as high as that of the other Wnts (Fig. 4B, *bottom panel*).

Ror2 did not bind Wnt7b under our experimental conditions. Thus, Ror2 shows specificity in its interactions with Wnts.

When Ror2 is immunoprecipitated out of U2OS extracts, it has the ability to phosphorylate itself *in vitro* (see Fig. 3C), presumably due to its intrinsic tyrosine kinase activity. We asked whether coexpression of Wnts affects the extent of Ror2 autophosphorylation. U2OS cells were transiently transfected with Ror2 in the presence of Wnt1, Wnt3, or a control plasmid, and the whole-cell extracts were isolated 24 h later. Ror2-flag was immunoprecipitated on flag affinity agarose followed by *in vitro* phosphorylation in the presence of ^{32}P-ATP. Figure 5A shows an autoradiograph followed by Western immunoblot of the same membrane. In Fig. 5B, results of at least three independent experiments were quantitated using Quantity One 1-D Image Analysis Software, and the radioactive signals were normalized to the total amount of immunoreactive Ror2 present in each reaction. There was no significant difference in Ror2 autophosphorylation in the absence or presence of Wnt1 or -3, indicating that these Wnts do not appear to affect Ror2 kinase activity. However, we cannot assess the stoichiometry of the immunoprecipitated complexes, and the amount of Wnts in these complexes may represent only a fraction of the amount of Ror2, thus obscuring the effects of Wnts on the Ror2 autophosphorylation.

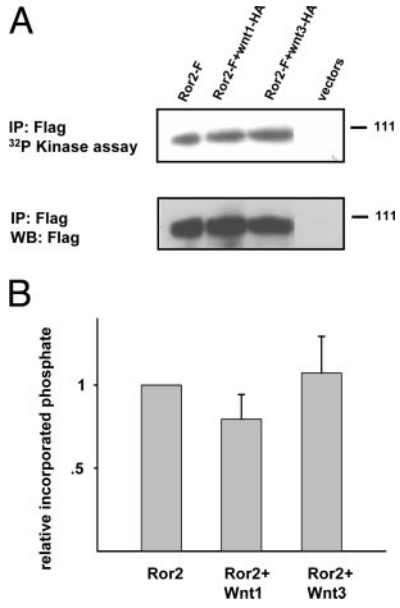

Fig. 5. Overexpression of Wnt1 and Wnt3 Has No Effect on the Extent of Ror2 Autophosphorylation

A, The *top panel* shows an autoradiograph of the results of *in vitro* autophosphorylation assay performed as described in *Materials and Methods* using Ror2-flag immunoprecipitated on flag affinity agarose out of U2OS cells cotransfected with Ror2-flag, the indicated Wnts, or pUSEamp and pcDNA3.1(+) (vectors). The *bottom panel* shows Western immunoblotting of the same membrane with antiflag antibody. B, Autoradiographic signals were normalized to the total amount of immunoreactive Ror2 protein in each reaction, and the relative signal obtained in the absence of Wnts was set at 1. The data are presented as means ± SE of three independent experiments.

To assess whether binding of Ror2 can affect Wnt signaling, we used a luciferase reporter assay that measures activation of the canonical Wnt pathway. Enzymatic activity of a luciferase reporter gene containing 16 copies of the Wnt-responsive TCF binding site was stimulated more than 20-fold after cotransfection of U2OS cells with Wnt3 construct (Fig. 6A). Ror2 by itself had no effect on promoter activity, but it inhibited Wnt3-induced activation. sFRP1 suppressed Wnt3 activity, and together sFRP1 and Ror2 suppressed it even further. By contrast, when the same promoter was activated by Wnt1, Ror2 potentiated

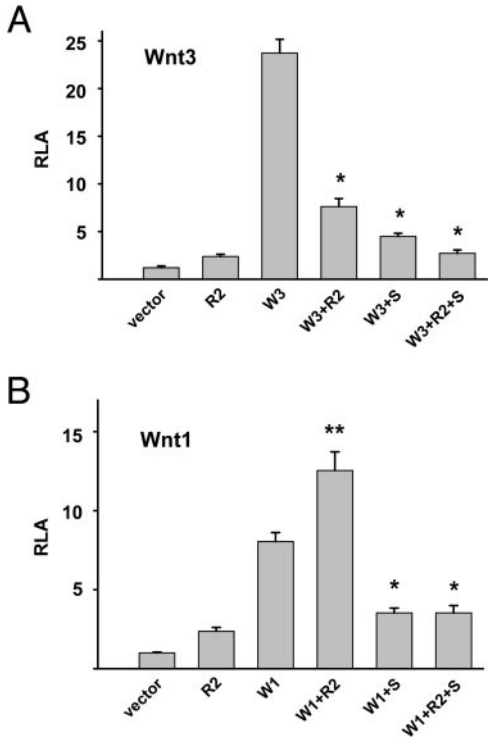

Fig. 6. Ror2 Inhibits Wnt3, But Potentiates Wnt1 Activity

U2OS cultures were transiently transfected with a recombinant luciferase reporter gene containing 16 copies of the TCF binding site cloned 5′ to the thymidine kinase promoter. In panel A, the promoter-reporter gene was cotransfected with pcDNA3.1(+) (vector), Ror2 (R2), Wnt3 (w3), or Wnt3 plus Ror2 (40 ng per well of a 96-well plate) or sFRP1 (S) or both. In panel B, the promoter-reporter gene was cotransfected with pcDNA3.1(+), Wnt1 (w1), or Wnt1 plus Ror2 (2.5 ng per well of a 96-well plate) or sFRP1, or both. The transfections were performed and relative luciferase activity (RLA) was measured as described in *Materials and Methods*. Luciferase values measured after transfection of a reporter gene in the presence of pcDNA3.1(+) have been arbitrarily given a value of 1. The data are presented as means ± SE of at least three independent experiments with $24 \leq n \leq 32$. The *asterisks* indicate significant changes in luciferase activity compared with the levels obtained with Wnt alone (*, significantly lower than Wnt; **, significantly higher than Wnt; $P < 0.001$).

Wnt1 activity (Fig. 6B). Once again, addition of sFRP1 overcame this potentiation and inhibited luciferase activity (Fig. 6B). To assess whether the effects of Ror2 were concentration dependent, we performed the TCF promoter-luciferase reporter assay in the presence of increasing amounts of the Ror2 plasmid (Fig. 7). In Fig. 7, the TCF promoter activity observed in the presence of Wnt alone was set at 100% and the Ror2-induced changes were plotted as functions of Ror2 concentration. Cotransfection with Ror2 inhibited, in a dose-dependent manner, Wnt3-induced activation of the promoter with an IC_{50} = 5.8 ng/well and a maximum suppression of 68% (Fig. 7A). In contrast, the effect on Wnt1 activity was biphasic with maximal potentiation of 140% at 2–10 ng/well (Fig. 7B).

To confirm that the observed promoter activity was regulated through Wnt-responsive lymphoid-enhancer binding factor/TCF transcription factors, we repeated the dose-response experiments with the well-characterized TOPflash TCF promoter and mutant FOPflash promoter. Both Wnt3 and Wnt1 potentiated the TOPflash (9- and 4-fold, respectively), but not the FOPflash promoter (data not shown). Ror2 potentiated Wnt1 in a dose-dependent manner but inhibited Wnt3-induced TOPflash activation (Fig. 8), confirming the results obtained on the 16xTCF promoter. In contrast, Ror2 did not potentiate FOPflash activity in the presence of Wnt1, nor inhibited it in the presence of Wnt3 (data not shown).

To confirm that the effect of Ror2 on the Wnt-responsive promoter was mediated through Ror-Wnt interactions, we performed luciferase reporter assays using Ror2 lacking the CRD domain. Consistent with the loss of 70% of Wnt3 binding (Fig. 4A), Ror2ΔCRD lost approximately 60% of its ability to inhibit Wnt3 signaling. Indeed, it achieved a maximal suppression of Wnt3 signaling of only 28% with an IC_{50} of 15.7 ng/well (Fig. 7A). Ror2ΔCRD failed to bind Wnt1 (Fig. 4A) and did not potentiate Wnt1 signaling at all concentrations tested (Fig. 7B). Thus, Wnt binding corre-

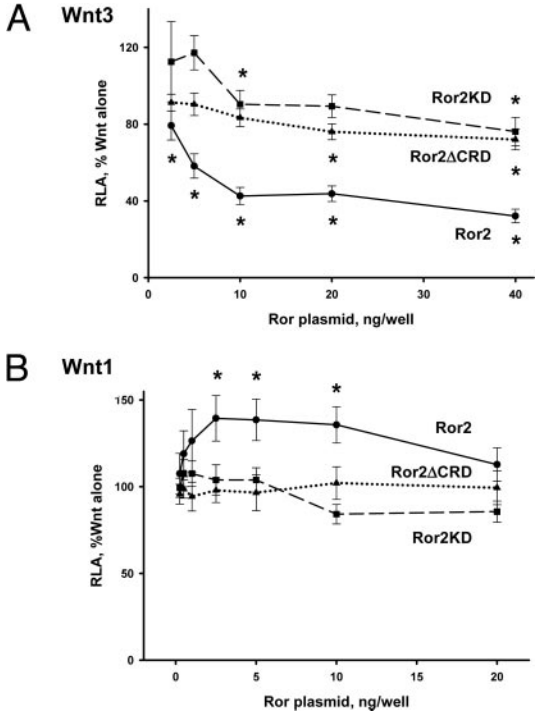

Fig. 7. Loss of Wnt Binding or Tyrosine Kinase Activity Impairs the Ability of Ror2 to Modulate Wnt Signaling

The U2OS cells were cotransfected with the TCF promoter-luciferase reporter gene and Wnt3 (A) or Wnt1 (B) in the presence of increasing amounts of the indicated Ror2 plasmids. Relative luciferase activity (RLA) was assessed as described in *Materials and Methods*, and the TCF promoter activity observed in the presence of Wnts alone was set at 100%, and the Ror2-induced changes were plotted as functions of Ror2 concentration. The *dashed curves* were obtained when Ror2KD was used in place of Ror2 and the *dotted lines* were obtained using Ror2ΔCRD. The data are presented as means ± SE of at least three independent experiments with 12≤n≤32. The *asterisks* indicate significant changes in luciferase activity compared with the levels obtained with Wnt alone ($P < 0.05$).

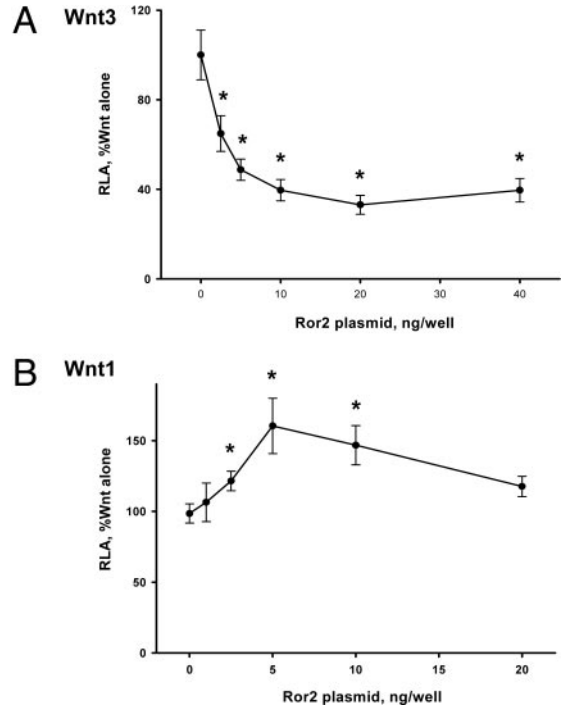

Fig. 8. Ror2 Inhibits Wnt3, But Potentiates Wnt1 Activity on the TOPflash Promoter

The U2OS cells were cotransfected with the TOPflash promoter-luciferase reporter gene and Wnt3 (A) or Wnt1 (B) in the presence of increasing amounts of the Ror2 plasmid. Relative luciferase activity (RLA) was assessed as described in *Materials and Methods*, and the TOPflash promoter activity observed in the presence of Wnts alone was set at 100% and the Ror2-induced changes were plotted as functions of Ror2 concentration. The data are presented as means ± SE of at least three independent experiments with n = 12. The *asterisks* indicate significant changes in luciferase activity compared with the levels obtained with Wnt alone ($P < 0.05$).

lates well with the ability of Ror2 to modulate activity of a Wnt-responsive promoter.

To investigate whether Ror2 kinase activity is required for modulation of Wnt signaling, we performed a luciferase reporter assay in the presence of increasing concentrations of the Ror2KD point mutant that has no tyrosine kinase activity. Despite the fact that Ror2KD construct expresses at about the same level as wild-type Ror2 (Fig. 3B), the kinase domain mutant did not potentiate Wnt1 signaling to the TCF promoter (Fig. 7B) and only inhibited Wnt3-induced activation of the promoter by about 24% (Fig. 7A). Thus, the tyrosine kinase activity of Ror2 is required for potentiation of Wnt1 signaling and for approximately 60% of Wnt3 inhibition.

As shown in Fig. 9A, Ror1 inhibited signaling by Wnt3, with an IC_{50} of 9.6 ng/well and a maximum inhibition of 56%. Given that in immunoprecipitation experiments, Ror1 appears to bind Wnt3 more weakly than does Ror2ΔCRD, some other downstream effects must explain the stronger ability of Ror1 to inhibit Wnt3 signaling to the promoter. Consistent with its lack of Wnt1 binding, addition of Ror1 at any dose examined had no effect on Wnt1-stimulated transcription (Fig. 9B), nor did Ror1 by itself have any effect on the TCF promoter activity (data not shown).

To address where in the canonical Wnt pathway that Ror2 functions, we assessed the ability of the Ror2 kinase to affect Wnt-mediated stabilization of cytosolic β-catenin. Upon transfection of Wnt1 or -3 into U2OS cells, the cytoplasmic levels of β-catenin increased by 1.6- or 2.4-fold, respectively (Fig. 10). Both increases, although modest, were reproducible in at least three independent experiments. Cotransfection with increasing amounts of Ror2 inhibited, in a dose-dependent manner, the ability of both Wnt1 and Wnt3 to stabilize cytosolic β-catenin. Ror2 by itself had no effect on β-catenin levels at all concentrations tested (data not shown). Interestingly, the kinase-dead Ror2 mutant was as potent as Ror2 in inhibiting β-catenin stabilization, indicating that the kinase activity is not required for this effect. Thus, Ror2-induced inhibition of Wnt3 signaling on the TCF promoter can be due, at least in part, to degradation of β-catenin. However, Ror2 must potentiate Wnt1 signaling on the TCF promoter by acting downstream of β-catenin stabilization. Furthermore, this additional arm of Ror2 signaling has to overcome the Ror2-induced decrease in β-catenin levels.

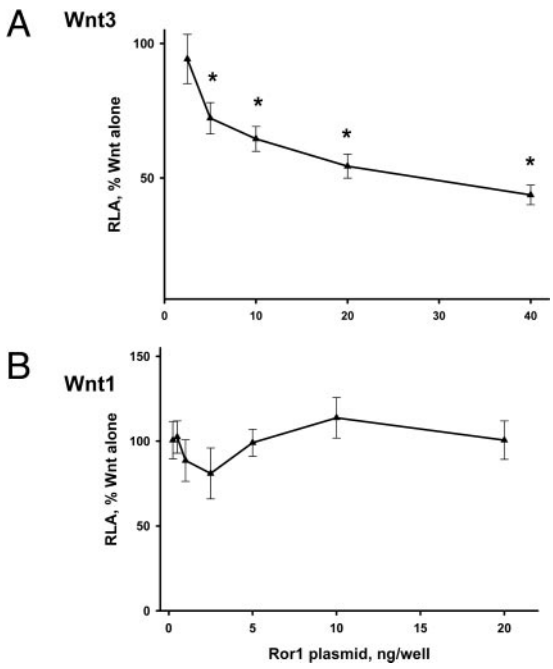

Fig. 9. Ror1 Inhibits Wnt3, But Has No Effect on Wnt1 Activity

The experiments were performed as in Fig. 7, except Ror1 was used in place of Ror2. The data are presented as means ± SE of at least three independent experiments with 24≤n≤32. The *asterisks* indicate significant changes in luciferase activity compared with the levels obtained with Wnt alone ($P < 0.001$). RLA, Relative luciferase activity.

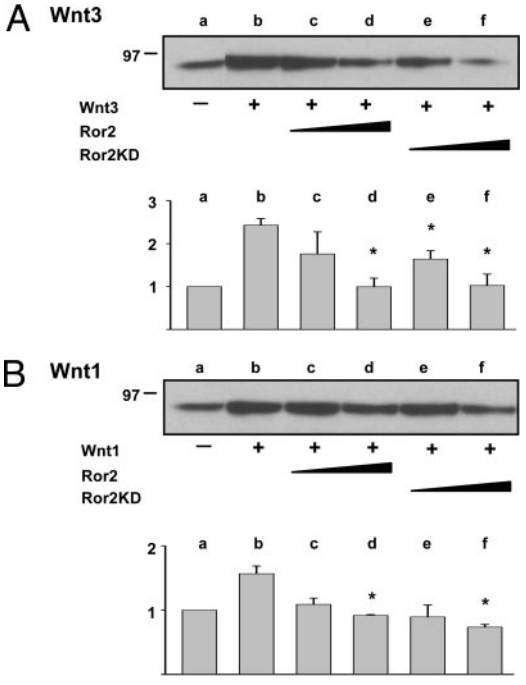

Fig. 10. Ror2 Inhibits Wnt-Mediated Stabilization of Cytosolic β-Catenin

U2OS cultures were transiently transfected with pcDNA (lane a), Wnts (lane b), or Wnts plus increasing amounts of Ror2 (lanes c and d) or Ror2KD (lanes e and f). The total amount of DNA was kept constant by addition of pcDNA3.1(+) in place of Ror. At 24 h, cytoplasmic proteins were analyzed by Western immunoblotting with anti-β-catenin antibody. The *bar graphs in each panel* present a summary of at least three independent experiments (means ± SE). Densitometric analysis was performed using Quantity One 1-D Image Analysis Software, the levels of β-catenin were normalized to the levels of β-actin in the same extracts, and the signal obtained in absence of Wnts was set at 1.

DISCUSSION

Our current studies show that Ror2 receptor tyrosine kinase modulates canonical Wnt signaling pathways. Furthermore, we identify Ror2 as a possible regulator of osteoblast survival and differentiation. Indeed, we show that 1) Ror2 is expressed in human osteoblasts and is strongly regulated during their differentiation, peaking in committed proliferating preosteoblasts; 2) Ror2 modulates canonical Wnt signaling pathway that regulates survival and differentiation of osteoblastic cells; and 3) Ror2 expression is suppressed by an antagonist of Wnt signaling and inhibitor of bone formation, sFRP1.

Real-time RT-PCR revealed that Ror2 expression was undetectable in human mesenchymal stem cells, increased 300-fold as they differentiated into committed preosteoblasts, and then declined sharply and disappeared in osteocytes. Previously, postnatal expression of Ror2 has been assessed in mouse bones by replacing the tyrosine kinase domain of the receptor with the LacZ gene (7). The β-galactosidase (β-gal) staining was found in articular cartilage and a subset of growth plate chondrocytes, but not in the bone tissue itself (7). Furthermore, the observed widespread skeletal abnormalities of the Ror2-null mice, including dwarfism, short limbs and tails, and facial defects, can be explained by the displayed defects in proliferation, maturation, and function of chondrocytes (7). Here, in addition to finding Ror2 expression in human osteoblastic cell lines, we used real-time RT-PCR to verify Ror2 expression in primary human osteoblasts and in mouse calvarial bones.

Here we show, for the first time, physical and functional interactions between the human Ror2 and the mammalian Wnts of the canonical family including Wnt1, -3, and -3a. The physical binding was demonstrated by immunoprecipitation out of the whole-cell extracts of U2OS or COS7 cells overexpressing full-length Ror2 and Wnts. Previously, the bacterially expressed extracellular domain of mouse Ror2 has been shown to bind a member of the noncanonical Wnt family, Wnt5a, but failed to bind the canonical Wnt3a *in vitro* (24). The lack of Wnt3a binding observed previously could be due to structural differences between human and mouse Ror2 receptors or it could result from differences in experimental conditions. In support of our data, the extracellular domain of the *Xenopus* Ror2 was shown to bind not only the noncanonical *Xenopus* Wnts 5a and 11, but also the canonical Wnt8 (23). Surprisingly, Ror2 retained some of its Wnt3 binding in the absence of the CRD domain. Deletion of the CRD domain has been shown to abolish Wg binding to Fz4 (31) and Wnt1 binding to sFRP3 (29), and several three-amino acid insertions into the CRD domain of DFz2 abolished binding of XWnt8 (30). However, to date, no information has been available on the Ror2 domains mediating Wnt interactions. We cannot exclude the possibility that Wnt3-Ror2ΔCRD binding seen here is nonspecific; however, under our experimental conditions Wnt1 did not bind Ror2ΔCRD and Wnt3 bound Ror1 extremely weakly. Our data seem to suggest that a portion of Ror2-Wnt3 binding may be mediated through non-CRD domains of Ror2 or through forming a complex with other, possibly CRD-containing, proteins.

The functionality of the Ror2-Wnt interactions observed here was demonstrated by the ability of Ror2 to modulate canonical Wnt signaling monitored by activation of the TCF promoter and stabilization of β-catenin. So far, Ror2 has been shown to potentiate the noncanonical Wnt signaling pathways: the c-Jun N-terminal kinase pathway in mice (24) and the planar cell polarity pathway in *Xenopus* (23). The ability of Ror2 to modulate the canonical Wnt signaling is of particular importance in osteoblastic cells, where the canonical pathway potentiates proliferation and activity (17). A role for noncanonical Wnt signaling in osteoblast function has not been firmly established, although it has been suggested based on the observed disparities in bone phenotypes of mice lacking canonical Wnt mediator (LRP5) *vs.* mice deficient in general Wnt inhibitor (sFRP1) (20). It is especially intriguing that Ror2 has opposing effects on Wnt1- and Wnt3-dependent promoter activation, potentiating Wnt1, but antagonizing Wnt3. To our knowledge, this is the first factor reported to have the opposite effects on Wnt1 and Wnt3 activity. Because Ror2 binds both Wnts and down-regulates β-catenin, the molecular basis for this discrimination must lie elsewhere in the pathway (see later).

Our results indicate that the tyrosine kinase activity of Ror2 is required for its ability to potentiate Wnt1 signaling and accounts for approximately 60% of its inhibitory activity against Wnt3 signaling. Conflicting evidence exists on the role of the tyrosine kinase activity in Ror2 signaling. Mice lacking the entire Ror2 receptor (6) and those lacking only the tyrosine kinase domain (7) appear to have indistinguishable phenotypes, indicating that Ror2 has no residual activity in the absence of the tyrosine kinase. Similarly, in humans, point mutations in the Ror2 tyrosine kinase domain cause Robinow syndrome as severe as that caused by deletion of almost the entire protein (8). On the other hand, in *Xenopus* (23) and *Caenorhabditis elegans* (32, 33) the extracellular domain of the Ror receptor has been shown to have some function independent of the tyrosine kinase activity. The simple explanation for this would be that Ror acts by binding Wnt and sequestering it away from its receptor, but Ror2 extracellular domain lacking the membrane-anchoring portion was inactive in *Xenopus*, indicating that an additional function of Ror2, perhaps as a cell adhesion molecule, is required for signaling (23).

Figure 11 presents a working model for modulation of canonical Wnt signaling by Ror2. Ror2 binds Wnt1 and Wnt3 and sequesters them away from their FZ receptors, resulting in increased degradation of β-catenin. This process does not require the tyrosine kinase activity of the Ror2 receptor. In addition, Wnt1 binding to Ror2 activates a Ror2 kinase-dependent signaling pathway that ultimately results in potentiation of TCF promoter activity. The fact that Wnt binding does not appear to modulate the Ror2 kinase

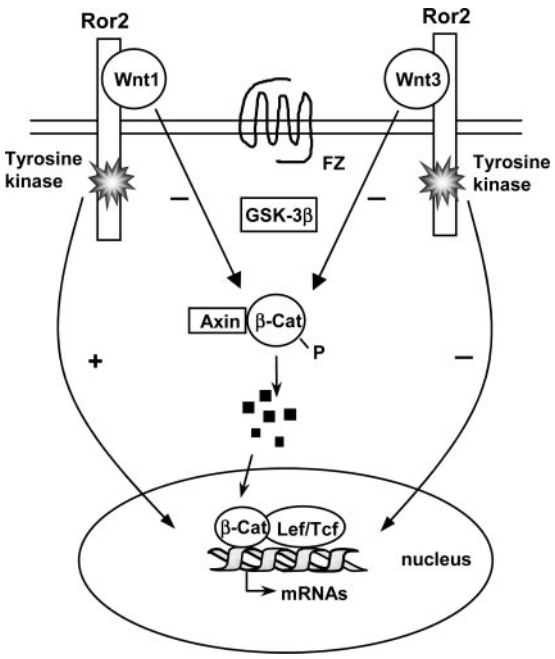

Fig. 11. Differential Effects of Ror2 on Wnt1 and Wnt3 Signaling

A proposed model for Ror2 activity whereby Ror2 binds both Wnts, sequestering them away from Frizzled receptors and inhibiting their ability to stabilize β-catenin. In addition, Wnt1 binding to the Ror2 receptor causes activation of an unidentified signaling cascade that requires tyrosine kinase activity of the Ror2 receptor and results in potentiation of Wnt-responsive promoter activity. Wnt3 binding does not stimulate the same cascade, but instead activates other tyrosine kinase-dependent events that lead to inhibition of Wnt-responsive promoters. FZ, Frizzled receptor; GSK-3β, glycogen synthase kinase β; β-cat, β-catenin; Lef/Tcf, lymphoid-enhancer binding factor/T cell transcription factor.

activity suggests that Wnt1 initiates some other event necessary for Ror2 activation, *e.g.* receptor dimerization or other events, and that the background level of Ror2 autophosphorylation is sufficient for its function. Wnt3 binding does not appear to activate this additional signaling pathway, and Ror2 inhibits Wnt3 activity on the TCF promoter. However, additional and at least partially kinase-dependent events downstream of β-catenin are required for this inhibition, because kinase-dead Ror2 antagonizes β-catenin stabilization, but loses 60% of its ability to inhibit the TCF promoter. Thus, the net effect of Ror2 on Wnt signaling is determined by the particular Wnts expressed by the cell.

As more evidence emerges positioning Ror2 in the Wnt signaling pathways, the important question arises of whether Ror2 can function independently of Wnt. Mutations in the Wnt-binding CRD domain of *Xenopus* Ror2 disrupt its function (23), and the single-point mutations in the CRD domain of human Ror2 result in Robinow syndrome indistinguishable from that caused by deletions of almost the entire protein (8), indicating that Wnt binding is required for the Ror2 function. However, it is possible that these mutations do not disrupt binding of at least some Wnts, but instead disrupt binding of a different, yet unidentified, Ror2 ligand or affect the three-dimensional structure of Ror2 and thus its function. In addition, recent published evidence proposes an alternative signaling mechanism for the Ror2 receptor. Ror2 has been shown to associate with and regulate nuclear localization of Dlxin-1 (34), which is known to modulate transcriptional activity of homeodomain proteins Msx2 and Dlx5. Intriguingly, abundant evidence exists that both Msx2 and Dlx5 modulate osteoblast differentiation (35–38), suggesting a mechanism by which Ror2 can control osteoblast differentiation independently of Wnt signaling.

In summary, our results demonstrate that Ror2 is expressed in human osteoblasts and is highly regulated during their differentiation. Our studies uncover the complex interactions between Ror2 and the canonical Wnt pathway that promotes osteoblast survival and differentiation. Because Ror2 has the ability to both inhibit and potentiate Wnt activity depending on the cellular context, additional studies will have to unravel the net effect of Ror2 signaling on osteoblast survival, differentiation, and function.

MATERIALS AND METHODS

Materials and Cells

Except where noted, tissue culture reagents were purchased from Invitrogen Corp. (Carlsbad, CA); other reagents and chemicals were purchased from either Sigma Chemical Co. (St. Louis, MO) or Invitrogen. Antiflag M2 mouse monoclonal antibody and antiflag M2 affinity agarose were obtained from Sigma; anti-HA tag and anti-β-catenin rabbit polyclonal antibodies and antiphosphotyrosine mouse monoclonal antibody, clone 4G10, were from Upstate Cell Signaling Solutions (Charlottesville, VA); anti-β-actin mouse monoclonal antibody was from Sigma; horseradish peroxidase-conjugated secondary antibodies were purchased from Santa Cruz Biotechnology, Inc. (Santa Cruz, CA) or Amersham Biosciences (Buckinghamshire, UK).

The U2OS human osteosarcoma cells were cultured in a 5% CO_2-95% humidified air incubator at 37 C using McCoy's 5A Modified Medium containing 10% heat-inactivated fetal bovine serum (HI FBS) and 1% penicillin-streptomycin (PS). COS7 cells were cultured at 37 C using DMEM containing 10% HI FBS and 1% PS.

Cloning and Plasmids

HA epitope-tagged Wnts in pUSEamp, pUSEamp(+), and TOPflash and FOPflash TCF reporter plasmids were obtained from Upstate Biotechnology, Inc. (Lake Placid, NY); pcDNA3.1(+) was from Invitrogen; cytomegalovirus (CMV) promoter-driven β-gal reporter gene (pCMVβ) was from BD Biosciences CLONTECH (Palo Alto, CA).

Luciferase reporter gene containing 16 copies of the TCF DNA binding site fused 5′ to a minimal thymidine kinase promoter (16xTCF-luc) was constructed by Dr. Ramesh A. Bhat (Wyeth Research). It contained four tandem copies of the following sequence incorporating four TCF DNA binding sites: 5′-CTAGCGAGAACAAAGGAGATTCAAAGGAGATCAAAGGAGATCAAAGGACTAGTTC-3′.

Flag-tagged human Ror1 was constructed as follows. The human Ror1 was cloned by Invitrogen from human uterus RNA and inserted into *Kpn*I and *Not*I sites of pcDNA3.1(+) to

obtain hRor1-pcDNA3. This clone was further modified by PCR-mediated mutagenesis to contain the flag epitope tag at the 3′-end of cDNA before the stop codon.

Flag-tagged human Ror2 was made as follows. The partial clone for human Ror2 containing the codons 58–2296 was obtained from Invitrogen's IMAGE clone collection (clone ID 3146587). The 3′-portion (codons 2297–2832) and the first 57 codons were produced by RT-PCR using HOB-03-C5 human osteoblast RNA as a template and Ror2-specific primers. After the entire coding region was verified by sequencing, the flag epitope tag was added to the 3′-end of hRor2 cDNA before the stop codon.

The Flag-tagged Ror2 kinase domain (Ror2KD) mutant diagrammed in Fig. 3A was constructed by PCR-mediated mutagenesis. The three-point mutations of lysines 507, 510, and 512 to isoleucines were introduced into Ror2-pcDNA3 using the QuikChange XL Site-Directed Mutagenesis Kit (Stratagene, La Jolla, CA) according to the manufacturer's instructions. The top-strand primer containing the intended mutations (*bold*) was: 5′-GGCTGTGGCCATCA**T**AACGCT-GA**TA**GACA**T**AGCGGAGGGGC-3′, and the bottom-strand primer was complementary to the top: 5′-GCCCCTCCGCT-**A**TGTC**TA**TCAGCGTT**A**TGATGGCCACAGCC-3′.

The Flag-tagged Ror2 mutant lacking the CRD domain (Ror2ΔCRD) diagrammed in Fig. 3A was obtained from Ror2-pcDNA by PCR-mediated mutagenesis. The 5′-portion of Ror2 (bp 1–519) was amplified by PCR using the top-strand primer containing the *Kpn*I site (*underlined*) and the ATG codon (*bold*) 5′-GACCTT*GGTACC***ATG**GCCCGGGGCTCG-GCGCT-3′ and the bottom strand primer containing the *Sph*I site (*underlined*) 5′-AGGTC*GCATGC*AGAACCCATCCTCGT-GGTAATCATC-3′. The 3′-portion was cut out of Ror2-pcDNA3 using an internal *Sph*I site at the 3′-end of the CRD domain. This strategy removed the entire CRD domain except for the last residue (C300).

RNA Analysis

Gene chip analysis of HOB cell lines and calvarial bones of sFRP1 knockout mice has been described previously (20, 26, 27). Primary human osteoblasts and the HOB cell lines were generated and maintained as described (39–43). Total cellular RNA was obtained using TRizol reagent (Invitrogen) per the manufacturer's protocol. hMSCs (BioWhittaker, Inc., San Diego, CA) were maintained at 37 C in phenol red-free DMEM medium containing 10% HI FBS and 1% PS (growth medium). Cells were seeded at 3100/cm^2 in six-well plates and 24 h later (d 0) the medium was changed for fresh growth medium or osteogenic medium (0.1 μM dexamethasone, 0.05 mM ascorbic acid, and 10 mM β-glycerophosphate in growth medium) for 21 d. Every 7 d, the total cellular RNA was isolated using RNeasy mini kit (QIAGEN, Valencia, CA) and the protocol of the manufacturer. RNA from primary human osteoblasts, HOB cell lines, and hMSC were subjected to real-time RT-PCR using the ABI PRISM 7700 Sequence Detection System (Applied Biosystems, Foster City, CA) according to the manufacturer's instructions. Sequences of primers and probes used are listed in Table 1. Probes were obtained from Applied Biosystems and labeled with the reporter fluorescent dye FAM. Primers and probe labeled with the reporter fluorescent dye VIC, specific for human 18S rRNA or human or rodent glyceraldehyde-3-phosphate dehydrogenase mRNA, were purchased from Applied Biosystems and used in the same or parallel reaction as an internal control. The RT step was performed at 48 C for 30 min, and the cDNA was amplified for 40 cycles at the following conditions: 95 C for 15 sec and 60 C for 1 min. The mRNA amount for each gene was calculated using the Standard Curve Method (Applied Biosystems) and normalized to the expression of 18S rRNA.

Alkaline Phosphatase and Osteocalcin Assays

hMSCs were seeded at 3100/cm^2 in 96-well plates and treated with growth medium or osteogenic medium for 21 d as for RNA analysis. Alkaline phosphatase activity and osteocalcin secretion were assessed every 3 d as previously described (42).

Reporter Gene Analysis

The U2OS cells were plated at 6.25 $\times$ 10^4/cm^2 in 96-well plates and transfected 24 h later with Lipofectamine 2000 transfection reagent (Invitrogen) per the protocol of the manufacturer. Combinations of the following DNAs were used [total DNA adjusted to 230 ng per well with pcDNA3.1(+)]: 180 ng 16xTCF-luc or TOPflash or FOPflash; 5 ng Wnt1 or Wnt3; 15 ng SFRP1; 5 ng pCMVβ; and the indicated amounts of Ror plasmids. Cells were lysed 24 h after transfection, and extracts were assayed for luciferase activity using the Luciferase Assay Reagent (Promega) and for β-gal activity using Galacto-Light (Applied Biosystems) as described by the manufacturers. Light emission was measured by MicroLumat LB 96P luminometer (EG&G Berthold, Bandoora, Australia) by integration over 10 sec for luciferase and 5 sec for β-gal. The light emission values obtained for luciferase were normalized to those for β-gal.

Table 1. Primers and Probes Used in the Real-Time RT-PCR Analysis

Kinase	Sequence (5′–3′)
Human Ror1	
Forward primer, 2993–3013	GTCGACTAGCACTGGCCATGT
Reverse primer, 3049–3074	CATGTGTGGTAGTAAAGGAATATTTGC
Probe, 3018–3044	AGCTTGCCCTCATCAGGATCCAATCAG
Human Ror2	
Forward primer, 1149–1169	CGTACGCATGGAACTGTGTGA
Reverse primer, 1239–1259	CAAGCGATGACCAGTGGAATT
Probe, 1174–1198	CCCTCGTGTAGTCCCCGAGACAGCA
Mouse Ror1	
Forward primer, 2350–2370	CCCCGATTTCCCAATTACATG
Reverse primer, 2402–2421	GCCAATGAAACCAGCGATCT
Probe, 2373–2395	CCCGAGCCAAGGGATTACACCCC
Mouse Ror2	
Forward primer, 364–386	ATCCAAGACCTGGACACAACAGA
Reverse primer, 429–448	GAACCCCAGTGGCAGTGATG
Probe, 400–424	TCAGCCCGTTGGTAGCCACACACTG

Transient Transfections and Western Immunoblotting

U2OS or COS7 cells were plated at approximately 90% confluent density and transfected 24 h later with 40 μg of total plasmid DNA per 143 cm^2 using FuGENE 6 transfection reagent (Roche Molecular Biochemicals, Indianapolis, IN) according to instructions of the manufacturer. After 24 h, cells were solubilized in lysis buffer [150 mM NaCl; 50 mM Tris-HCl, pH 7.5; 1 mM EDTA; 1% Triton X100; protease and phosphatase inhibitor cocktails (both from Sigma)], and the extracts were clarified by centrifugation at 500,000 $\times$ *g* for 30 min at 4C. For assessing β-catenin stabilization, U2OS cells were plated at 90% confluent density in six-well plates and transfected 24 h later using 6.9 μg of total plasmid DNA and Lipofectamine 2000 transfection reagent following manufacturer's protocol. After 24 h, the cytoplasmic protein extracts were prepared by solubilization in hypotonic buffer [10 mM Tris-HCl, pH 7.4; 200 μM $MgCl_2$; protease and phosphatase inhibitor cocktails (both from Sigma)] followed by 40 passes in Dounce homogenizer and centrifugation at 100,000 $\times$ *g* for 90 min at 4 C. For immunoblotting, 50 μg of total cell lysate protein or 19 μg of cytoplasmic extract were resolved by SDS-PAGE under denaturing and reducing conditions before transfer onto nitrocellulose membranes and Western immunoblotting with specific antibodies.

Immunoprecpitation and *in Vitro* Autophosphorylation Assay

U2OS cells were transfected as for Western immunoblotting, and 24 h later solubilized in kinase lysis buffer [150 mM NaCl; 50 mM Tris-HCl, pH 7.5; 1% Triton; 20 mM NaF; 2 mM sodium vanadate; protease inhibitor cocktail without EDTA (Sigma); 250 μM phenylmethylsulfonyl fluoride]. The extracts were clarified by centrifugation at 500,000 $\times$ *g* for 30 min at 4 C. Total cell lysate protein (1 mg) was incubated with 50 μl of M2 flag affinity agarose (Sigma) for 1 h with rotation at 4 C. The beads were collected by centrifugation, washed three times in kinase lysis buffer containing 350 mM NaCl and three times in kinase lysis buffer, and used for Western immunoblotting or autophosphorylation assays. For the Westerns, the beads were boiled in 50 μl of 2$\times$ LDS-PAGE buffer with reducing agent (Invitrogen), and the solubilized proteins were separated by SDS-PAGE. The gels were transferred onto nitrocellulose membrane before detection with each specific antibody. For the autophosphorylation assays, the beads were washed two times in kinase reaction buffer (10 mM $MgCl_2$; 50 mM Tris-HCl, pH 7.5; 1 mM dithiothreitol). Where indicated, 10% of the beads were set aside for SDS-PAGE analysis followed by silver staining with SilverQuest kit (Invitrogen). The rest of the beads were resuspended in 50 μl of kinase reaction buffer containing 1 mM ATP and 15 μCi [γ-^{32}P] ATP. The kinase reaction was allowed to proceed for 30 min at 30 C and stopped by boiling in 1$\times$ LDS buffer plus reducing agent (Invitrogen). Proteins were resolved by SDS-PAGE, transferred onto nitrocellulose membranes, and exposed to x-ray film for 12 h. Where indicated, the membrane was subsequently probed with antiflag antibody as described in *Western Immunoblotting*, and images were quantitated using Quantity One 1-D Image Analysis Software (Bio-Rad Laboratories, Inc., Hercules, CA).

Statistical Analysis

Data are presented as means $\pm$ SE. Statistical significance was determined using Student's *t* test. Results were considered statistically different when $P < 0.05$.

Acknowledgments

We thank Dr. Ramesh A. Bhat and Mrs. Barbara Stauffer for providing the 16xTCF-luc construct.

Received April 15, 2004. Accepted September 16, 2004.

Address all correspondence and requests for reprints to: Julia Billiard, Ph.D., Women's Health Research Institute, Wyeth Research, 500 Arcola Road, Collegeville, Pennsylvania 19426. E-mail: billiaj@wyeth.com.

REFERENCES

1. Forrester WC 2002 The Ror receptor tyrosine kinase family. Cell Mol Life Sci 59:83–96
2. Matsuda T, Nomi M, Ikeya M, Kani S, Oishi I, Terashima T, Takada S, Minami Y 2001 Expression of the receptor tyrosine kinase genes, Ror1 and Ror2, during mouse development. Mech Dev 105:153–156
3. Oishi I, Takeuchi S, Hashimoto R, Nagabukuro A, Ueda T, Liu ZJ, Hatta T, Akira S, Matsuda Y, Yamamura H, Otani H, Minami Y 1999 Spatio-temporally regulated expression of receptor tyrosine kinases, mRor1, mRor2, during mouse development: implications in development and function of the nervous system. Genes Cells 4:41–56
4. Al-Shawi R, Ashton SV, Underwood C, Simons JP 2001 Expression of the Ror1 and Ror2 receptor tyrosine kinase genes during mouse development. Dev Genes Evol 211: 161–171
5. Nomi M, Oishi I, Kani S, Suzuki H, Matsuda T, Yoda A, Kitamura M, Itoh K, Takeuchi S, Takeda K, Akira S, Ikeya M, Takada S, Minami Y 2001 Loss of mRor1 enhances the heart and skeletal abnormalities in mRor2-deficient mice: redundant and pleiotropic functions of mRor1 and mRor2 receptor tyrosine kinases. Mol Cell Biol 21:8329–8335
6. Takeuchi S, Takeda K, Oishi I, Nomi M, Ikeya M, Itoh K, Tamura S, Ueda T, Hatta T, Otani H, Terashima T, Takada S, Yamamura H, Akira S, Minami Y 2000 Mouse Ror2 receptor tyrosine kinase is required for the heart development and limb formation. Genes Cells 5:71–78
7. DeChiara TM, Kimble RB, Poueymirou WT, Rojas J, Masiakowski P, Valenzuela DM, Yancopoulos GD 2000 Ror2, encoding a receptor-like tyrosine kinase, is required for cartilage and growth plate development. Nat Genet 24:271–274
8. Afzal AR, Jeffery S 2003 One gene, two phenotypes: ROR2 mutations in autosomal recessive Robinow syndrome and autosomal dominant brachydactyly type B. Hum Mutat 22:1–11
9. Afzal AR, Rajab A, Fenske CD, Oldridge M, Elanko N, Ternes-Pereira E, Tuysuz B, Murday VA, Patton MA, Wilkie AO, Jeffery S 2000 Recessive Robinow syndrome, allelic to dominant brachydactyly type B, is caused by mutation of ROR2. Nat Genet 25:419–422
10. van Bokhoven H, Celli J, Kayserili H, van Beusekom E, Balci S, Brussel W, Skovby F, Kerr B, Percin EF, Akarsu N, Brunner HG 2000 Mutation of the gene encoding the ROR2 tyrosine kinase causes autosomal recessive Robinow syndrome. Nat Genet 25:423–426
11. Schwabe GC, Tinschert S, Buschow C, Meinecke P, Wolff G, Gillessen-Kaesbach G, Oldridge M, Wilkie AO, Komec R, Mundlos S 2000 Distinct mutations in the receptor tyrosine kinase gene ROR2 cause brachydactyly type B. Am J Hum Genet 67:822–831
12. Oldridge M, Fortuna AM, Maringa M, Propping P, Mansour S, Pollitt C, DeChiara TM, Kimble RB, Valenzuela DM, Yancopoulos GD, Wilkie AO 2000 Dominant mutations in ROR2, encoding an orphan receptor tyrosine kinase, cause brachydactyly type B. Nat Genet 24: 275–278
13. Wodarz A, Nusse R 1998 Mechanisms of Wnt signaling in development. Annu Rev Cell Dev Biol 14:59–88
14. Huelsken J, Birchmeier W 2001 New aspects of Wnt signaling pathways in higher vertebrates. Curr Opin Genet Dev 11:547–553

15. Huelsken J, Behrens J 2002 The Wnt signalling pathway. J Cell Sci 115:3977–3978
16. Veeman MT, Axelrod JD, Moon RT 2003 A second canon. Functions and mechanisms of β-catenin-independent Wnt signaling. Dev Cell 5:367–377
17. Patel MS, Karsenty G 2002 Regulation of bone formation and vision by LRP5. N Engl J Med 346:1572–1574
18. Gong Y, Slee RB, Fukai N, Rawadi G, Roman-Roman S, Reginato AM, Wang H, Cundy T, Glorieux FH, Lev D, Zacharin M, Oexle K, Marcelino J, Suwairi W, Heeger S, Sabatakos G, Apte S, Adkins WN, Allgrove J, Arslan-Kirchner M, Batch JA, Beighton P, Black GC, Boles RG, Boon LM, *et al*. 2001 LDL receptor-related protein 5 (LRP5) affects bone accrual and eye development. Cell 107:513–523
19. Kato M, Patel MS, Levasseur R, Lobov I, Chang BH, Glass DA, 2nd, Hartmann C, Li L, Hwang TH, Brayton CF, Lang RA, Karsenty G, Chan L 2002 Cbfa1-independent decrease in osteoblast proliferation, osteopenia, and persistent embryonic eye vascularization in mice deficient in Lrp5, a Wnt coreceptor. J Cell Biol 157:303–314
20. Bodine PV, Zhao W, Kharode YP, Bex FJ, Lambert AJ, Goad MB, Gaur T, Stein GS, Lian JB, Komm BS 2004 The Wnt antagonist secreted frizzled-related protein-1 is a negative regulator of trabecular bone formation in adult mice. Mol Endocrinol 18:1222–1237
21. Saldanha J, Singh J, Mahadevan D 1998 Identification of a Frizzled-like cysteine rich domain in the extracellular region of developmental receptor tyrosine kinases. Protein Sci 7:1632–1635
22. Masiakowski P, Yancopoulos GD 1998 The Wnt receptor CRD domain is also found in MuSK and related orphan receptor tyrosine kinases. Curr Biol 8:R407
23. Hikasa H, Shibata M, Hiratani I, Taira M 2002 The *Xenopus* receptor tyrosine kinase Xror2 modulates morphogenetic movements of the axial mesoderm and neuroectoderm via Wnt signaling. Development 129:5227–5239
24. Oishi I, Suzuki H, Onishi N, Takada R, Kani S, Ohkawara B, Koshida I, Suzuki K, Yamada G, Schwabe GC, Mundlos S, Shibuya H, Takada S, Minami Y 2003 The receptor tyrosine kinase Ror2 is involved in non-canonical Wnt5a/JNK signalling pathway. Genes Cells 8:645–654
25. Bodine PV, Komm BS 2002 Tissue culture models for studies of hormone and vitamin action in bone cells. Vitam Horm 64:101–151
26. Billiard J, Moran RA, Whitley MZ, Chatterjee-Kishore M, Gillis K, Brown EL, Komm BS, Bodine PV 2003 Transcriptional profiling of human osteoblast differentiation. J Cell Biochem 89:389–400
27. Bodine PVN, Moran R, Ponce-de-Leon H, McLarney S, Green J, Stein GS, Lian JB and Komm BS 2001 Secreted frizzled-related protein (sFRP)-1: a novel regulator of osteoblast and osteocyte apoptosis. J Bone Miner Res 16:S168 (Abstract)
28. Masiakowski P, Carroll RD 1992 A novel family of cell surface receptors with tyrosine kinase-like domain. J Biol Chem 267:26181–26190
29. Lin K, Wang S, Julius MA, Kitajewski J, Moos Jr M, Luyten FP 1997 The cysteine-rich frizzled domain of Frzb-1 is required and sufficient for modulation of Wnt signaling. Proc Natl Acad Sci USA 94:11196–11200
30. Hsieh JC, Rattner A, Smallwood PM, Nathans J 1999 Biochemical characterization of Wnt-frizzled interactions using a soluble, biologically active vertebrate Wnt protein. Proc Natl Acad Sci USA 96:3546–3551
31. Bhanot P, Brink M, Samos CH, Hsieh JC, Wang Y, Macke JP, Andrew D, Nathans J, Nusse R 1996 A new member of the frizzled family from *Drosophila* functions as a Wingless receptor. Nature 382:225–230
32. Forrester WC, Dell M, Perens E, Garriga G 1999 A *C. elegans* Ror receptor tyrosine kinase regulates cell motility and asymmetric cell division. Nature 400:881–885
33. Kim C, Forrester WC 2003 Functional analysis of the domains of the *C elegans* Ror receptor tyrosine kinase CAM-1. Dev Biol 264:376–390
34. Matsuda T, Suzuki H, Oishi I, Kani S, Kuroda Y, Komori T, Sasaki A, Watanabe K, Minami Y 2003 The receptor tyrosine kinase Ror2 associates with the melanoma-associated antigen (MAGE) family protein Dlxin-1 and regulates its intracellular distribution. J Biol Chem 278:29057–29064
35. Acampora D, Merlo GR, Paleari L, Zerega B, Postiglione MP, Mantero S, Bober E, Barbieri O, Simeone A, Levi G 1999 Craniofacial, vestibular and bone defects in mice lacking the Distal-less-related gene Dlx5. Development 126:3795–3809
36. Satokata I, Ma L, Ohshima H, Bei M, Woo I, Nishizawa K, Maeda T, Takano Y, Uchiyama M, Heaney S, Peters H, Tang Z, Maxson R, Maas R 2000 Msx2 deficiency in mice causes pleiotropic defects in bone growth and ectodermal organ formation. Nat Genet 24:391–395
37. Holleville N, Quilhac A, Bontoux M, Monsoro-Burq AH 2003 BMP signals regulate Dlx5 during early avian skull development. Dev Biol 257:177–189
38. Cheng SL, Shao JS, Charlton-Kachigian N, Loewy AP, Towler DA 2003 MSX2 promotes osteogenesis and suppresses adipogenic differentiation of multipotent mesenchymal progenitors. J Biol Chem 278:45969–45977
39. Bodine PVN, Harris HA, Komm BS 1999 Suppression of ligand-dependent estrogen receptor activity by bone-resorbing cytokines in human osteoblasts. Endocrinology 140:2439–2451
40. Bodine PV, Komm BS 1999 Evidence that conditionally immortalized human osteoblasts express an osteocalcin receptor. Bone 25:535–543
41. Bodine PV, Vernon SK, Komm BS 1996 Establishment and hormonal regulation of a conditionally transformed preosteocytic cell line from adult human bone. Endocrinology 137:4592–4604
42. Bodine PVN, TrailSmith M, Komm BS 1996 Development and characterization of a conditionally transformed adult human osteoblastic cell line. J Bone Miner Res 11:806–819
43. Robey PG, Termine JD 1985 Human bone cells in vitro. Calcif Tissue Int 37:453–460

Molecular Endocrinology **is published monthly by The Endocrine Society (http://www.endo-society.org), the foremost professional society serving the endocrine community.**